Nuclear Physics **A500** (1989) 701–730
North-Holland, Amsterdam

MULTIPION DYNAMICS FOLLOWING ANTIPROTON ANNIHILATION ON NUCLEI

J. CUGNON, P. DENEYE and J. VANDERMEULEN

Université de Liège, Physique Nucléaire Théorique, Institut de Physique au Sart Tilman, Bâtiment B.5, B-4000 Liège 1, Belgium

Received 2 February 1989

Abstract: Extensive calculations based on our improved version of the intranuclear cascade model for antiproton annihilation in flight on atomic nuclei are presented and compared with experimental data in the LEAR regime. The relationship between the main features of the inclusive proton and pion cross sections and some specific aspects of the cascade dynamics is studied. The sensitivity of the results upon variation of the input data is investigated. In particular it is shown that limited knowledge of medium corrections on pion interactions and of nuclear-structure detail entails such an uncertainty on the predicted high-energy proton cross section that no firm conclusion on the possible signature for unusual phenomena can be drawn from the comparison with experiment. The charged pion multiplicity is particularly studied. The experimental data are reviewed and their inconsistency is underlined. The pion absorption mechanism is discussed in much detail and its influence on the pion yield is exhibited. Medium corrections are discussed. The role of the Δ-degrees of freedom is reanalyzed, and a way to test their relevance is proposed. Existing cascade models are compared with each other and the dispersion of the results is underlined.

1. Introduction

The bulk of the existing data on antiproton annihilation on nuclei, both at rest and in flight are grossly consistent with the intranuclear cascade (INC) picture of the interaction between the target nucleons and the pions issued from the annihilation of the antiproton with a single nucleon (for a recent review, see ref. [1])). The agreement is particularly good for the general features of the data, like e.g. the shape of the inclusive cross sections. Although the data are too scarce to allow good systematic studies and keeping in mind that the INC is still a rather crude model for the quantum multiple-scattering problem in spite of constant refinements, one has to find out whether detailed and specific parts of the data like tails of momentum spectra, target mass dependence, etc, are still consistent with the INC picture, whether they call for refinements of the cascade dynamics or whether they indicate the presence of unusual effects. This is the main goal of this paper.

Actually, our purpose is threefold: (i) we want to compare systematically the predictions of the INC model developed by our group with the experimental data for annihilation in flight in the LEAR regime (only fragmentary results have been shown in previous publications); (ii) we isolate whenever possible the relationship between selected parts of the data and specific aspects of the INC dynamics. In

addition, we want to study the sensitivity of the results upon modification of the input. This would help to determine whether quoted discrepancies are really indicative of the presence of unusual effects. Occasionally, we will also discuss the difference between various INC calculations; (iii) the dynamical picture of the pion absorption and propagation will be discussed in detail. In particular, we will reanalyze the role of the Δ-resonance and the adequacy of its description.

The paper is divided as follows. In sect. 2, we recall the features of our INC code. Sect. 3 is devoted to comparison with experiment concerning the inclusive measurements. We discuss the relationship between the different parts of the momentum spectra with various aspects of the model (primordial pions, singly hit nucleons, Fermi motion, ...). We study the sensitivity of our predictions under reasonable variations of the input of the INC model. Those variations are consistent with the uncertainty of some nucleon-nucleon, nucleon-pion or nuclear structure data or with expected medium effects. Sect. 4 is devoted to the absorption of pions which seems to be underestimated in our standard INC model. We particularly investigate the possible influence of some medium effects. A thorough discussion of the dynamical picture of the pion propagation and of the role of the Δ-resonance is presented. In particular, we point out that their presence can sizeably reduce the absorption. A possible experimental signature of this presence is discussed. In sect. 5, we compare the various INC models used for the antiproton-nucleus system. Sect. 6 contains a detailed analysis of our results and of their implications.

2. The intranuclear cascade model for antiproton annihilation

We stress again the basic features of the INC models [2-9]) used to describe antiproton annihilation on nuclei:

(i) the antiproton annihilates on a single nucleon generating at a well-defined point of space-time a few pions with the same characteristics as observed in free space;

(ii) the pions cascade through the nucleons, making collisions with the target nucleons, which can be ejected. They may also be absorbed or just leave without any interaction (see below);

(iii) after the fast ejection process has taken place, the remaining excitation energy, more or less randomized, is released by usual evaporation process.

Most of details of our INC model are extensively discussed in previous publications [6-9]). Let us however mention some improvements and recall some features which are important for the subsequent discussions.

The antiproton is assumed to follow a curved trajectory in the field created by the nucleus. We assume the latter is attractive, with the same Woods-Saxon geometry as the nuclear density. The depth is adjusted to reproduce the total annihilation cross sections. Its value is consistent with the optical-model fits of the elastic and reaction cross sections [10,11]). The attractive field bends the trajectory inward. As a

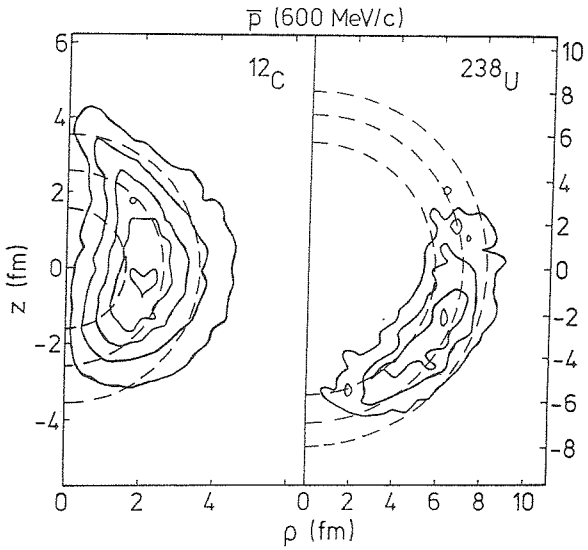

Fig. 1. Contour plot of the distribution of the annihilation site $d^2N/d\rho\, dz$ for 608 MeV/c antiprotons. The quantities ρ and z are the cylindrical coordinates relative to the beam axis (parallel to the beam and passing through the centre of the target). The dashed curves correspond to 10, 50 and 90% maximum density radii. The antiprotons are supposed to come from below.

result, the cross section increases by ~20%, compared to linear trajectory. Another consequence is that the distribution of the annihilation point is not restricted to the frontzone of the nucleus, but extends on the sides of the nucleus and even a little bit on the rear, in the case of very light targets (see fig. 1).

The pions issued from the annihilation (the primoridal pions) are given momentum according to phase space. The CERN program FOWL [12]) is used for this purpose. The number of pions is generated randomly according to a gaussian law with parameters given in ref. [13]). Their charge is chosen in agreement with the model of ref. [14]).

The multipion cascade is simulated by the method described in refs. [6-9]). The fate of all particles is followed *at the same time.* Particles travel along straight-line trajectories between collisions. These occur at the time of minimum relative distance if the latter is small enough, i.e. if the criterion

$$d \leqslant \sqrt{\sigma/\pi}\,, \tag{2.1}$$

is fulfilled, where σ is the appropriate cross section (this method is used also to determine the nucleon partner for the annihilation of the incoming antiproton). Baryons are reflected by the nuclear surface, if their kinetic energy is not large enough to escape [see ref. [9]) for detail].

The isospin degrees of freedom are included in the same way as for the INC model for heavy-ion collisions [see refs. [15,16]), where all detail concerning the elementary cross sections can be found].

In this work, we do not include the evaporation process [step (3) mentioned above] except for one particular case in sect. 3.2. This actually only affects the low-energy part of the proton spectra which is not our main interest here.

The following reactions are included:

$$\mathrm{NN} \to \mathrm{NN}, \quad \mathrm{NN} \leftrightarrows \mathrm{N}\Delta, \quad \Delta\Delta \to \Delta\Delta, \quad \mathrm{N}\Delta \to \mathrm{N}\Delta,$$
$$\pi\mathrm{N} \leftrightarrows \Delta, \quad \pi\mathrm{NN} \to \mathrm{NN}, \quad \pi\mathrm{N} \to \pi\mathrm{N}. \tag{2.2}$$

For most of the time, the pion absorption proceeds through the two step process

$$\pi\mathrm{N} \to \Delta, \quad \Delta\mathrm{N} \to \mathrm{NN}. \tag{2.3}$$

3. INC predictions; Comparison with experiment

3.1. INCLUSIVE PROTON AND PION CROSS SECTIONS

The most important piece of data is provided by the results of the PS187 experiment [3]): the π^+ and p angle-integrated momentum spectra for 608 MeV/c antiproton annihilations on ^{12}C and ^{238}U targets. They are shown in fig. 2 along with our predictions. Globally, the agreement is quite good, especially for the proton spectra. For the pion spectra, a distinctive feature of our results is the presence of a kind of (broad) dip around $p \approx 300$ MeV/c. Such a structure seems to be visible in the

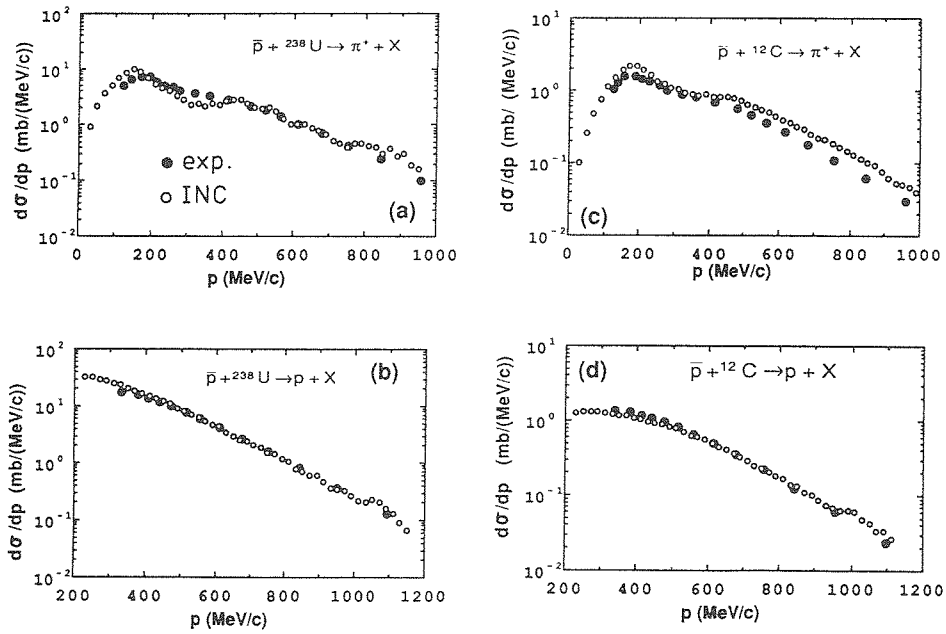

Fig. 2. Comparison between our INC results (open dots) and the experimental data (full dots) of ref. [3]) for inclusive π^+ and proton $\mathrm{d}\sigma/\mathrm{d}p$ cross sections.

C-data but not in the U-data. A closer look at our results reveals that we overestimate the pion yield (see later).

The data as well as our results can be plotted in another way in order to emphasize Maxwell–Boltzmann tails (fig. 3). The π^+ spectra clearly show two slopes, characterized by "temperatures". As stressed in ref. [17]), the large temperature component is dominated by the *noninteracting* pions, i.e. those pions issued from the annihilation that do not scatter on nucleons, a result which mainly stems from the peripheral nature of the annihilation. The lowest temperature component corresponds to rescattered pions. This is substantiated by fig. 4, where *in the calculation* we have isolated the contribution of the noninteracting pions and compared with the spectrum of the primordial pions. It can be seen that the final pions with momentum larger than ~400 MeV/c have practically not interacted.

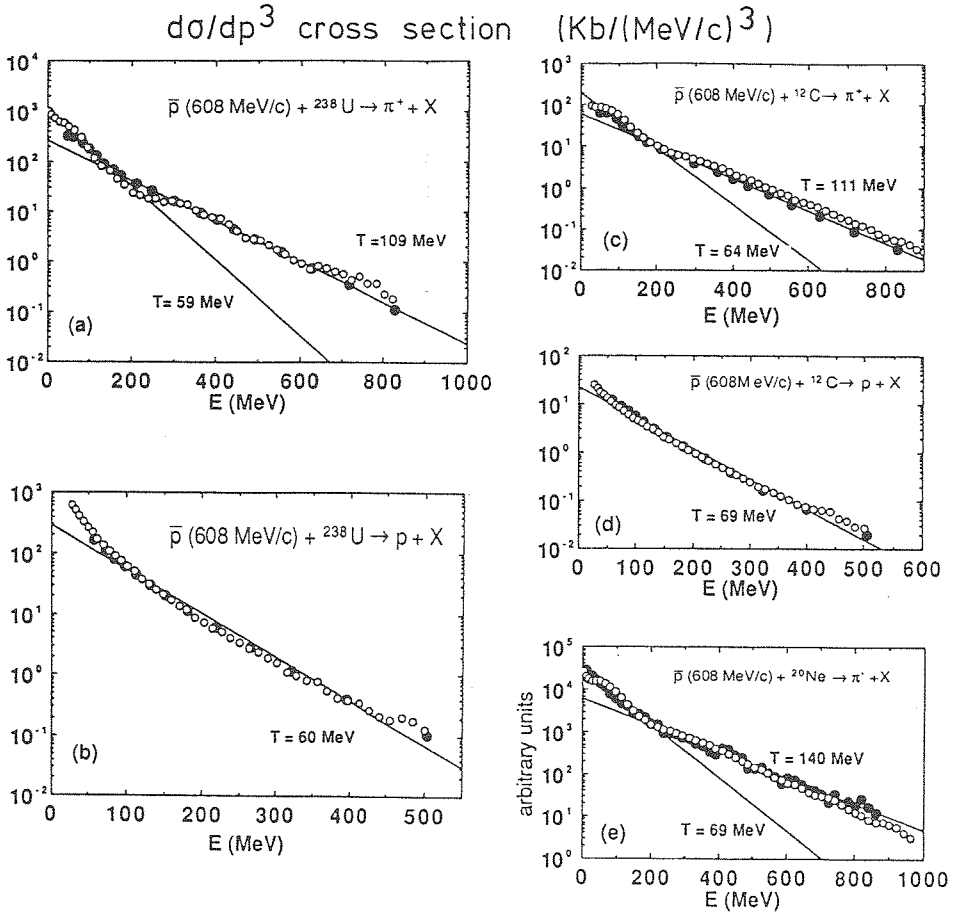

Fig. 3. Same as fig. 2 for the quantity $d\sigma/dp$. The π^- data for Ne target [28]) are shown (in arbitrary units). The straight lines give maxwellian fits of the data. See text for detail.

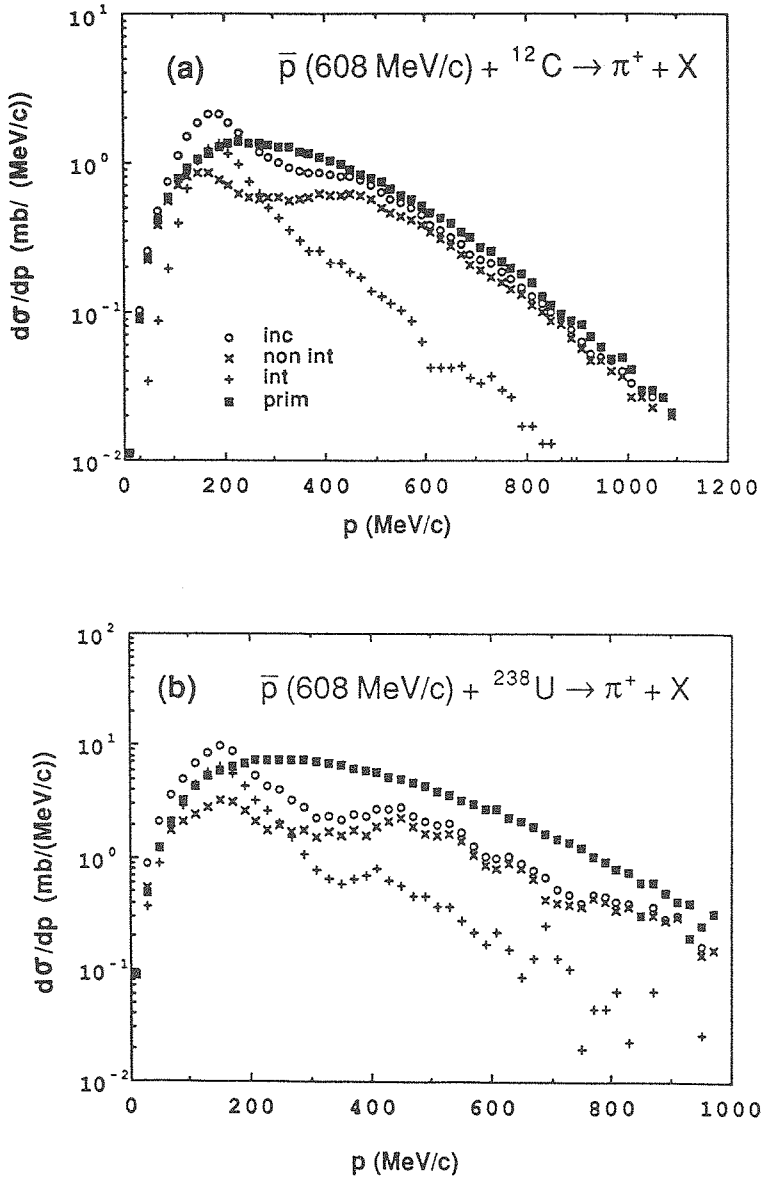

Fig. 4. Inclusive π^+ cross sections: INC results (open dots), primordial pion spectrum (squares), interacting pion contribution (+) and noninteracting pion contribution (×). See text for detail.

Close examination of fig. 4 tells that the shoulder observed in the pion spectrum comes from the interplay of the interacting and noninteracting pion contributions. The first has a maximum at ~180 MeV/c and the second one shows a minimum around 300 MeV/c, as a result of Δ-formation. Summing up the two contributions leads to the observed structure around ~350 MeV/c.

The calculated proton spectrum also shows two slopes. The "high temperature" one is associated with the nucleons which have been hit once by high-energy primoridal pions and with those issued from the pion absorption. We recall that the total pion energy is then transferred to two nucleons which so receive a rather high energy. This is illustrated in fig. 5 for the ^{12}C target, where it is shown that the proton yield above ~700 MeV/c is almost entirely due to the above-mentioned contributions. For lower momentum, the latter become less and less important. Therefore, it is expected that the second component (of lower temperature) is due to secondary protons. This is however not a precise denomination since we checked that this contribution arises from protons hit by a recoiling nucleon (after collision initiated by a primary pion) but also from protons hit by a pion having previously interacted. As emphasized in ref. [17]), the presence of maxwellian tails in energy spectra does not necessarily correspond to emission by a thermal source, i.e. by an equilibrated system with a well defined temperature. The high-energy tail in the π-spectrum has nevertheless this meaning, since it merely reflects the properties of the primordial pions, which are believed to correspond typically to a pion black-body

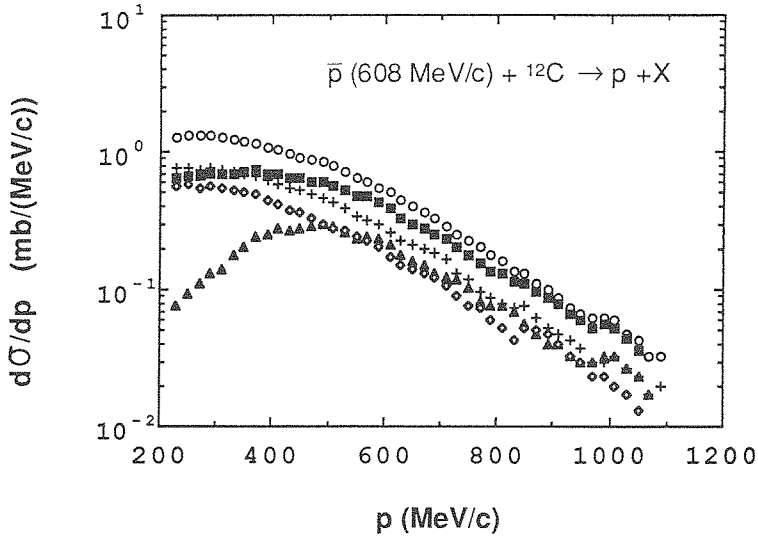

Fig. 5. Inclusive p cross sections. The INC prediction is given by the open dots. The open lozenges correspond to protons which have undergone a single hit by a pion. The contribution of the nucleons which have been involved in a pion absorption only is given by the triangles. The squares give the sum of the two latter contributions. The crosses include the protons which have been hit once only, either by a pion or by another baryon (nucleon or delta).

radiation with a temperature ~110 MeV. On the contrary, the high momentum tail of the proton spectrum basically results from the single interaction of thermal-like pions with nucleons. The same remark applies to the "low temperature" component of the pion spectrum. In conclusion, the multipion cascade does not seem to lead to the heating of a large part of the nucleus but rather resembles a multispallation process. Each interacting pion makes just a few collisions only [17,18]) (~2–5, depending upon the nuclear size) and ejects a few energetic particles (energetic in the sense of the domain investigated in the experiment). Of course, as in p- or π-induced spallation reactions, after the fast ejection process initiated by the incoming particle is over, the remaining energy is progressively randomized and the target emits slower and slower particles. Therefore, one expects an evaporation component at very low energy. For a light nucleus like C, this component could be visible in the proton spectrum, but will appear in neutron spectrum only for heavy targets. For a U-target, the fission is expected to compete with evaporation. This has been observed in antiproton annihilation at rest [19]).

The direct relationship between the high-energy tail of the primordial pions and the high-energy tail of the proton spectrum is also underlined by fig. 6. Here, we changed artificially the generation of the primordial pions in order to give them, so to speak, a lower temperature. This modified primordial spectrum appears to be very close to the one used in McGaughey *et al.* [3]). Obviously, the high-energy pion cross section is now depressed, giving rise to a decrease of the high-energy protons. The proton tail is sensitive to other effects, like the interaction model for high-energy pions. Most calculations somehow neglect these interactions, assuming only the tail of the Breit-Wigner contribution due to the Δ-resonance. However the π-nucleon system displays an important cross section above this resonance, especially in the $I = \frac{1}{2}$ state [20]). In the present calculation (as well as in ref. [9])), a constant cross section of ~30 mb is used above $\sqrt{s} = 1360$ MeV. In order to keep the calculation at a tractable level, we nevertheless adopt the same mechanism for the π-absorption as in the Δ-region. This may be somehow unrealistic but gives a rough picture of the interacting high-energy pions. To see the importance of this feature, we compare in fig. 7 the results obtained with a constant cross-section above the Δ-resonance with those obtained using a pure Breit-Wigner. The pion tail is slightly arising in the latter case, but the most important change is the strong decrease in the tail of the proton spectrum. The two curves can be considered as bracketing the results for a correct dynamical treatment of high energy pions.

The influence of the nuclear input data should also be investigated. In fig. 8, we look at the influence of the nucleon momentum distribution $g(k)$. In recent years, it has been conjectured [21–23]) that the latter could depart from a Fermi distribution, with adjunction of a high momentum tail. As an example, we used

$$\begin{aligned} g(k) &= Ak^2, & k < k_F, \\ &= B\, e^{-k/k_0}, & k > k_F. \end{aligned} \tag{3.1}$$

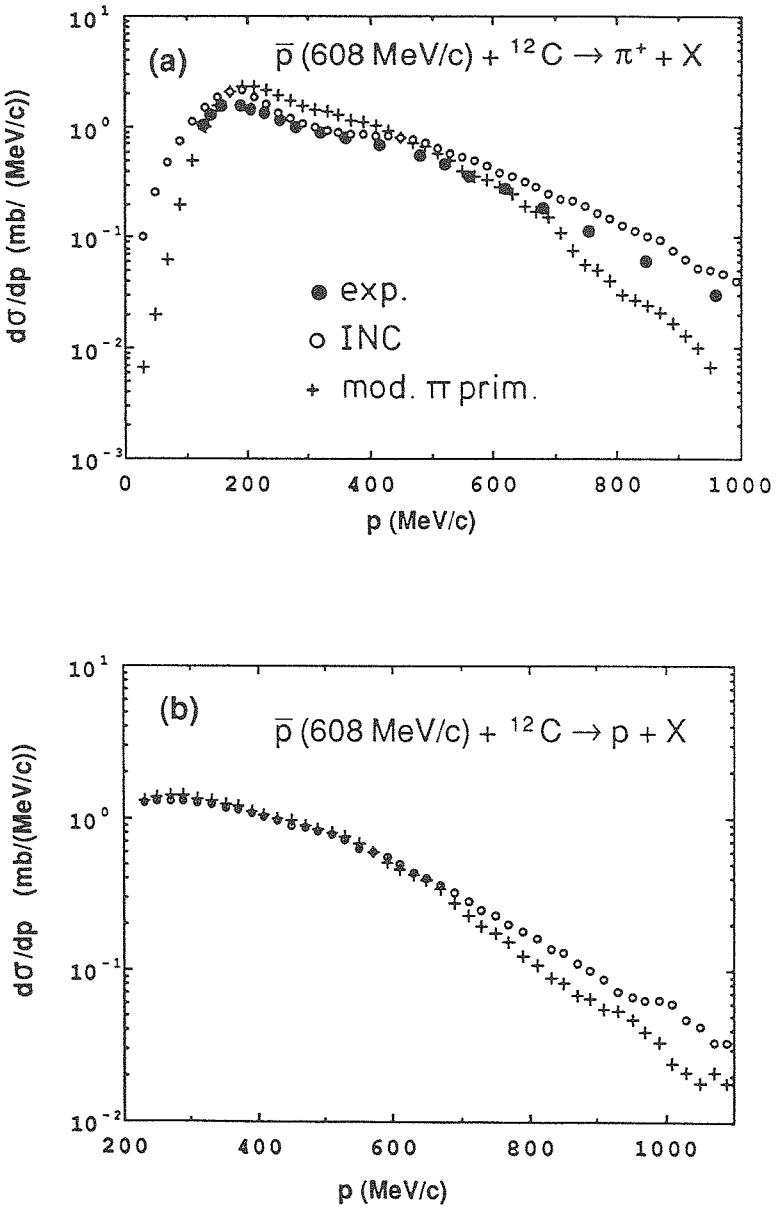

Fig. 6. Inslusive π^+ and p cross sections. Comparison between our standard INC results (open dots) and those obtained by using a narrower primordial pion spectrum (crosses), similar to the one used in ref. [3]). The experimental π^+ cross section (full dots) is also shown.

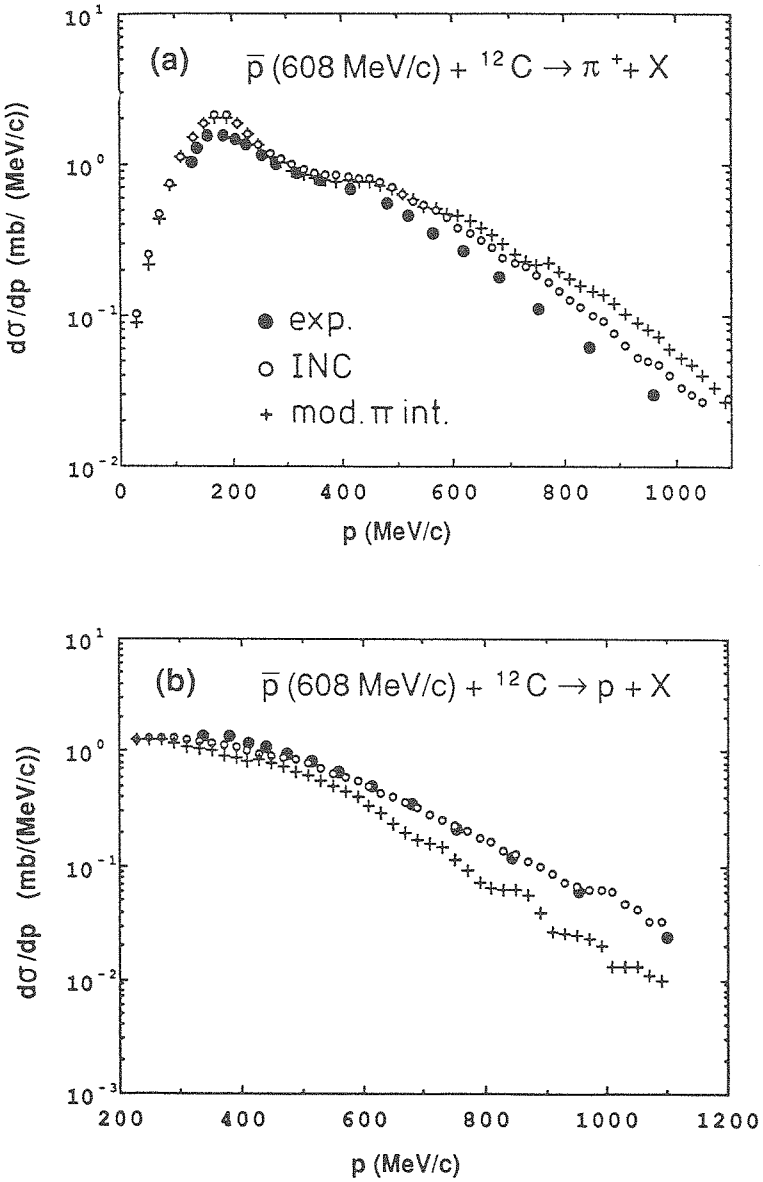

Fig. 7. Inclusive π^+ and p cross sections. Comparison between experiment (full dots), our standard INC results (open dots) and those obtained by modifying the interaction of high-energy pions. See text for detail.

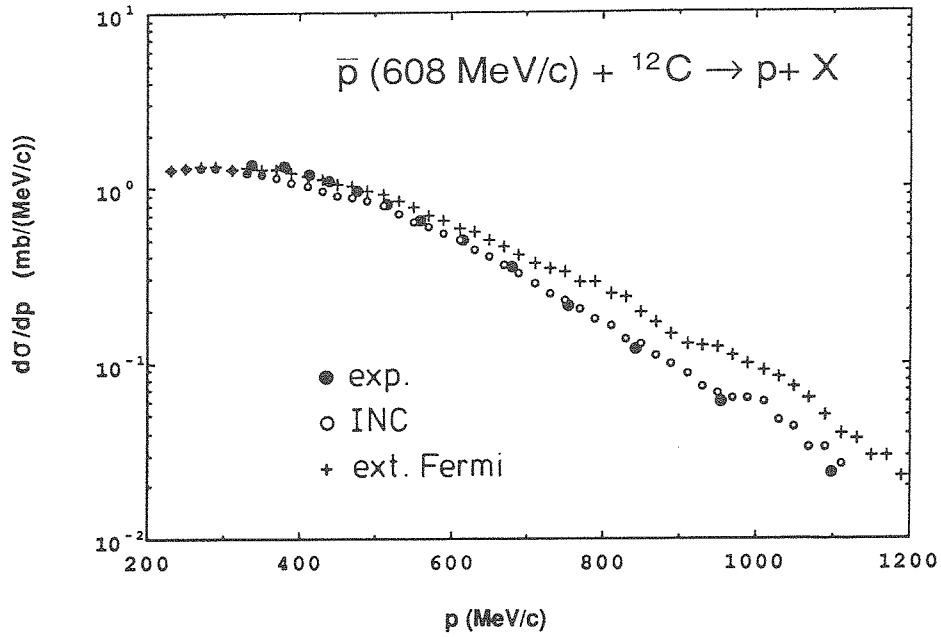

Fig. 8. Inclusive p cross section. Comparison between experiment (full dots), our standard INC results (open dots) and the one obtained by using a momentum distribution extending beyond the Fermi momentum (eq. (3.1)). See text for detail.

The parameters A, B and k_0 have been fixed to give a 25% depopulation of the Fermi sea and $\langle k \rangle \approx 2k_F$ in the tail, following recent claims [23-25]). As expected, the introduction of distribution (3.1) produces an important rise of the tail of the proton yield.

We want to stress here that the status of the actual calculations does not allow to take the predictions for the high energy tail of proton spectrum more seriously than within a factor 2 or 3. Therefore, in our opinion, it is premature to state, as it is done in refs. [26,27]) that the $\bar{p} + {}^{12}C \to p + X$ spectrum provides evidence for unusual phenomena.

3.2. THE Ne CASE

We consider this case separately for two reasons. First, it does not seem to follow the systematic behaviour based on the three targets ^{12}C, ^{89}Y and ^{238}U considered in ref. [3]). Second, the data are more detailed in some respect.

Fig. 9 compares the results of our standard cascade with the π^- data of ref. [28]). The overall agreement is satisfactory. However, several points are worth to be mentioned. As shown in fig. 3, the tail of the experimental spectrum ($p_\pi \approx$

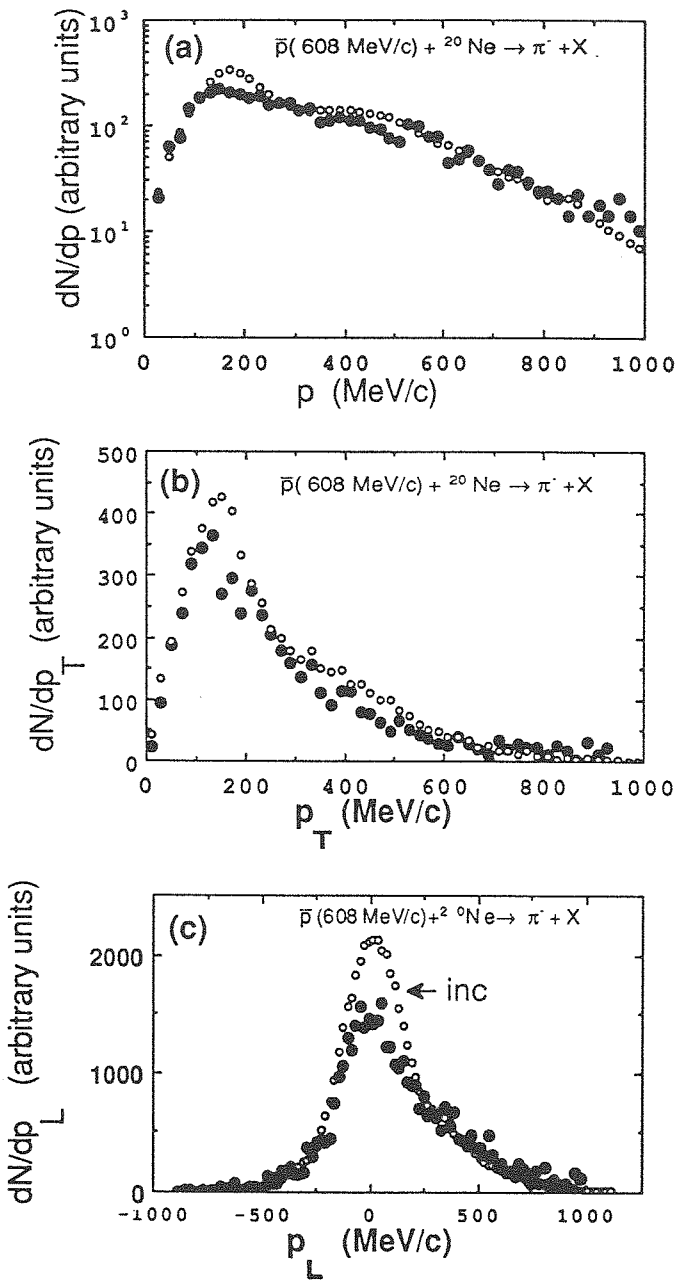

Fig. 9. Negative pion total (a), transverse (b) and longitudinal (c) momentum distribution following $\bar{p}$ annihilation on ^{20}Ne. Comparison between data (full dots) of ref. [28]) and our INC results (open dots).

500 MeV/c) displays a surprisingly large temperature, almost as large as the so-called Hagedorn temperature [29]). The calculation reproduces quite well the shape of the transverse distribution, but overestimates the longitudinal momentum distribution near $p_L \approx 0$. This seems to indicate some difficulty for the INC to account for absorption of slow pions (see sect. 4), or, possibly, some experimental loss of tracks in the $y \approx 0$ region.

A complementary information is contained in fig. 10, where the π^- angular distribution is displayed. The experimental data indicate a depression at $\cos\theta \approx 0$, corresponding to a strong differential absorption at $\theta \approx 90°$, i.e. of pions travelling transversally. Pions are emitted preferentially in the forward direction, a feature which may be contradictory to the common-belief of an annihilation occurring at the front of the nucleus followed by a total absorption of the pions travelling into the forward hemisphere. As was first pointed out in ref. [6]) and repeatedly acknowledged in the literature, the emission pattern of fig. 10 results from the moving annihilation frame, and a relatively strong transparency of nuclear matter with respect to high energy pions (above the Δ-resonance). Fig. 10 seems to indicate the INC underestimates this transparency.

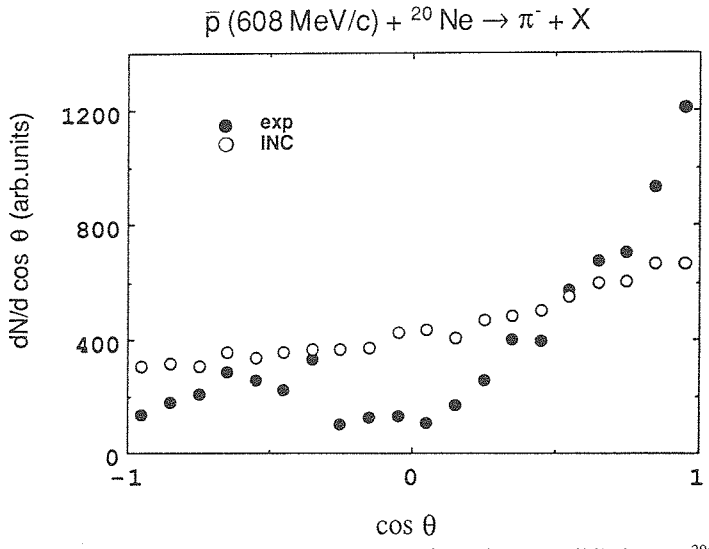

Fig. 10. Angular distribution of the negative pions emitted following p̄-annihilation on ^{20}Ne. The full dots are the data of ref. [28]) and the open dots are our results. The distributions have the same normalization.

For the antiproton-Ne case, many correlation measurements have been performed. Fig. 11 displays the average π^- multiplicity as a function of the charged particle multiplicity M observed in the detector (a streamer chamber in this case). There

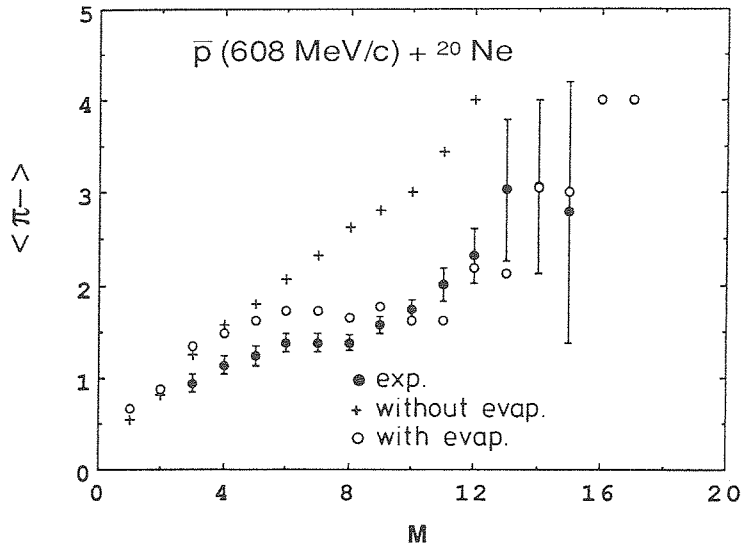

Fig. 11. Average π^- multiplicity as function of charged particle multiplicity (M). Comparison between data [28]) (full dots) and our INC results. The open dots correspond to the inclusion of evaporation whereas the crosses are obtained when the latter is neglected. See text for detail.

is, as usual in similar cases, some difficulty in comparing theory with experiment. The detector "sees" any charged particle (with some cuts and some efficiency) including sometimes heavy fragments while theory does not introduce easily a reliable fragmentation process. Charged particles include here charged pions, cascade protons, evaporated protons and heavier nuclear fragments, which may come from evaporation, but also from the cascade process (see ref. [30])). No information is available for the heavy-fragment yield in the ^{20}Ne case [28]). We expect very few of them and identify the multiplicity M with charged pions plus protons (cascade + evaporation). We use the same evaporation model as in ref. [9]). On the average, an evaporated nucleon removes 20 MeV of excitation energy. Our results are shown by the triangles in fig. 11. The cascade reproduces reasonably well the data but the correct shape is not at all obtained when the evaporation is not taken into account. This is of course in keeping with fig. 12, where the momentum spectrum for the emitted protons is shown. In contradistinction with ref. [3]), the experimental apparatus permits measurements below $\approx$300 MeV/c and thus an investigation of the evaporation component. Our INC calculations reproduce very well the spectrum for $p \geqslant 350$ MeV/c. The difference between data and the crosses in fig. 10 shows the importance of the evaporation component. After integration, one has $\sim$1.7 cascade protons and $\sim$2 evaporated protons. Our (too crude) evaporation model somehow overestimates the evaporation component. Coming back to the correlations described in fig. 11, the present INC model is in agreement with the simplified mean-free-path model described in ref. [31]).

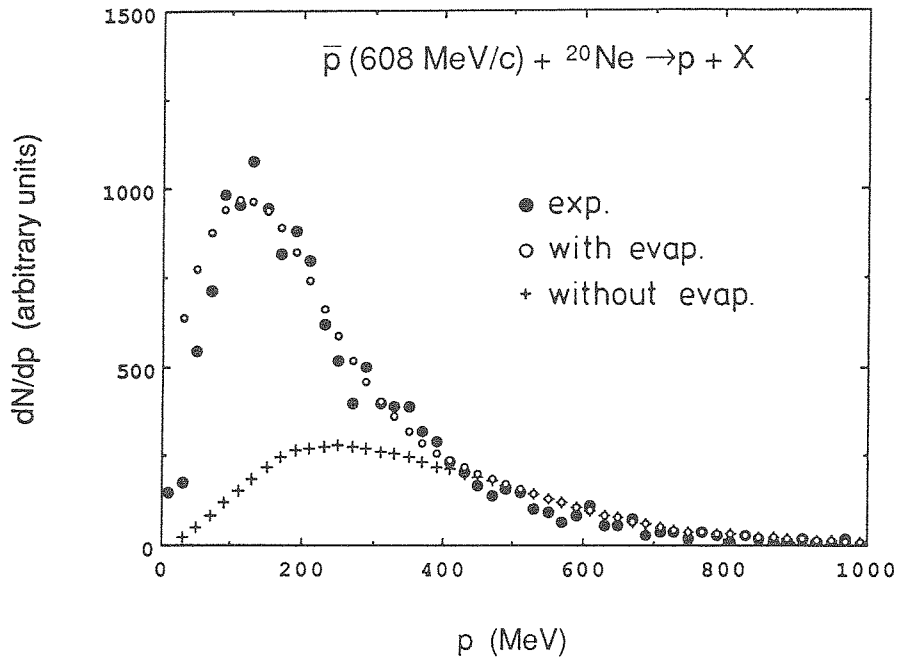

Fig. 12. Proton momentum spectrum for $\bar{p}$ annihilation events on ^{20}Ne target. Same symbol convention as in fig. 11.

In fig. 13, we show the correlation between the charged particle multiplicity M and the average π^- longitudinal momentum $\langle p_L \rangle$, the average cosine of the π^- emission angle and the total energy of the negative pions, respectively. One can see that the INC model explains the general trends. There are two discrepancies, however: (i) the $\langle p_L \rangle$ for small multiplicity is slightly underestimated; (ii) the π^- energy is overpredicted for intermediate multiplicity. A closer analysis (see sect. 4) indicates that the energy transfer per absorbed pion seems all right, but the absorption of pions is underestimated.

3.3. THE $\bar{n}$ ANNIHILATION DATA

Very few data of acceptable quality exist. A measurement has been performed [32]) with a $\bar{n}$ (1403 MeV/c) beam and a ^{12}C target. Fig. 14 gives the main data in comparison with our predictions. We see that the agreement is better than for the other cases. In particular, the proton as well as pion angular distributions are remarkably well reproduced.

A recent experiment has been performed [33]) on Fe target. Only the charged pion multiplicity has been measured. The data are rather puzzling, since they indicate a very small pion absorption (see fig. 15). We will come to this point in the next section.

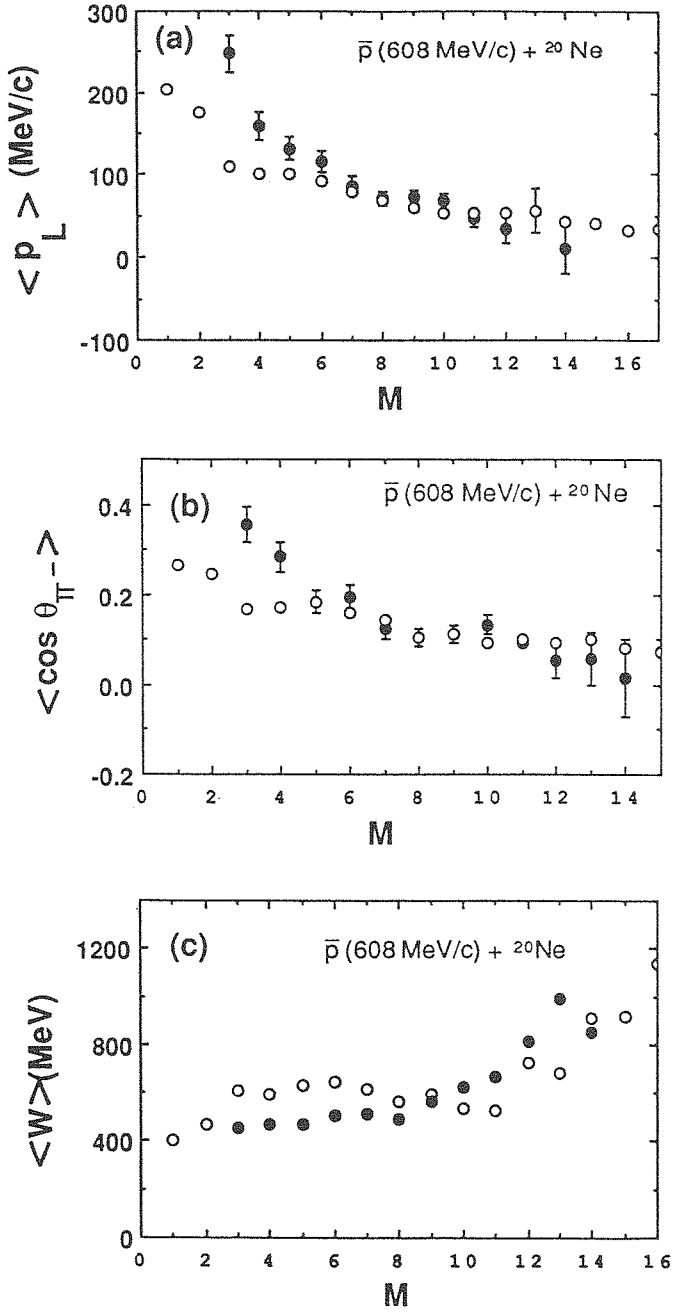

Fig. 13. Comparison between experimental data [28]) (full dots) and our INC results (open dots). The various quantities are respectively: the average longitudinal π^- momentum (a), the average cosine of the polar emission angle for the π^-'s (b) and the total energy (in the lab system) carried by the final π^-'s, for a given charged particle multiplicty M. See text for detail.

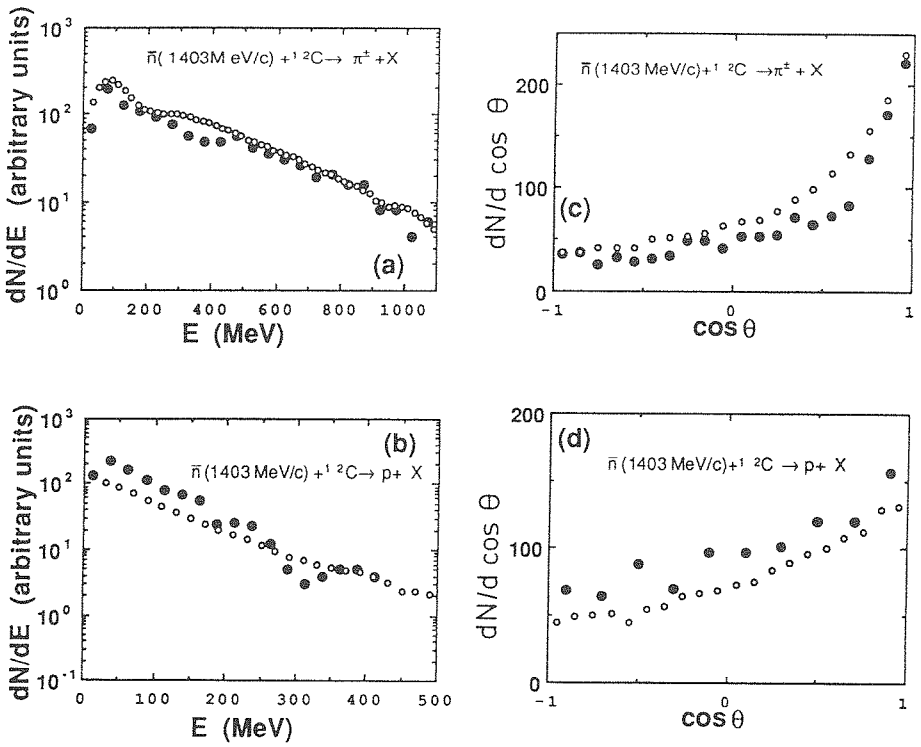

Fig. 14. Kinetic energy E spectrum and angular distribution for the negative pions and the protons emitted following annihilation of antineutrons on a ^{12}C target. Comparison between experimental data of ref. [32]) (full dots) and our results (open dots).

4. Pion multiplicities

4.1. GENERAL REMARKS

We have seen in sect. 3 that our standard INC model, as well as most of the other approaches, reproduces reasonably well the pion spectrum. This may not be surprising since e.g. the broadness of the pion spectrum is directly determined by the primordial pion spectrum. In other words, the *shape* of pion spectrum is not so sensitive to the detail of the multipion dynamics. This is no longer the case for the zeroth moment of the pion spectrum, i.e. the pion multiplicity, as we will see. The ability of a model to describe properly this multiplicity has not been discussed very much in the literature (see however sect. 6 of ref. [28])) and is not easily assessed from figures as fig. 2, when a broad spectrum is displayed in a semi-logarithmic plot.

4.2. REVIEW OF THE EXPERIMENTAL DATA

In fig. 16, we present the most complete data for a given antiproton momentum, namely the charged pion multiplicity around 600 MeV/c. To give an idea of the

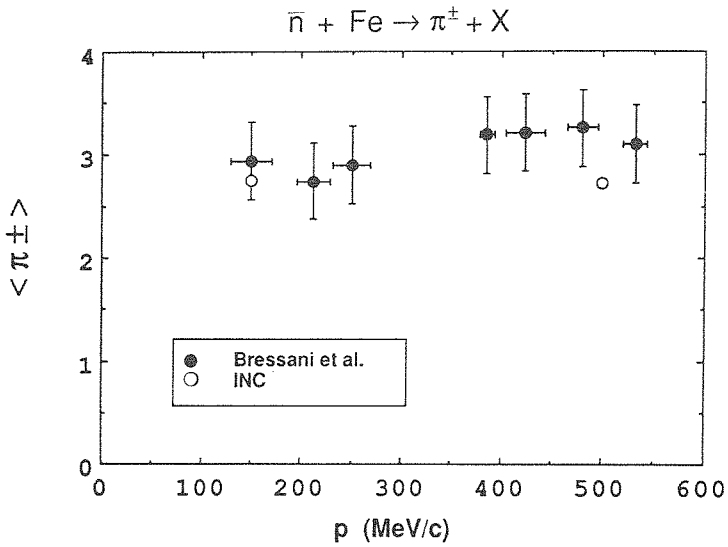

Fig. 15. Comparison between our results (open dots) and the data of ref. [33]) concerning the charged pion multiplicity for the $\bar{n}$-annihilation on Fe target as a function of the incident momentum p of the antineutron.

absorption, we have represented the evaluated primordial charged pion multiplicity, assuming the annihilation occurs as in free space, on a proton or a neutron in proportion to their numbers. The most striking feature of fig. 16a is the strong disagreement between the counter results of McGaughey *et al.* [3]) and the bubble chamber and emulsion data, especially for the ^{12}C data. The streamer chamber experiment for ^{20}Ne provides only the π^- multiplicity [28]). For this charge state, the streamer-chamber value is larger than the general trend of ref. [3]), although it cannot be stated that they strongly disagree.

For the sake of comparison, we also give in fig. 16b, the $\pi^\pm$ multiplicity for annihilation at rest. The absorption rate r_{abs}, defined as

$$r_{abs} = \frac{\langle \pi \rangle_{prim} - \langle \pi \rangle_{fin}}{\langle \pi \rangle_{prim}}, \tag{4.1}$$

is about half the value at 600 MeV/c. Presumably, this comes from the larger number of interacting pions in the latter case and to a lesser extent from the intrinsic absorption properties changing with kinematical conditions. On the basis of a mean free path, one expects a relation of this kind:

$$r_{abs} = \alpha_{int}[1 - \exp(-L_0 A^{1/3}/\lambda)], \tag{4.2}$$

where α_{int} is the fraction of interacting pions among the primordial ones (possibly dependent upon A). L_0 is some characteristic length, A is the mass number and λ the absorption mean free path. The restricted range of variation of A and the

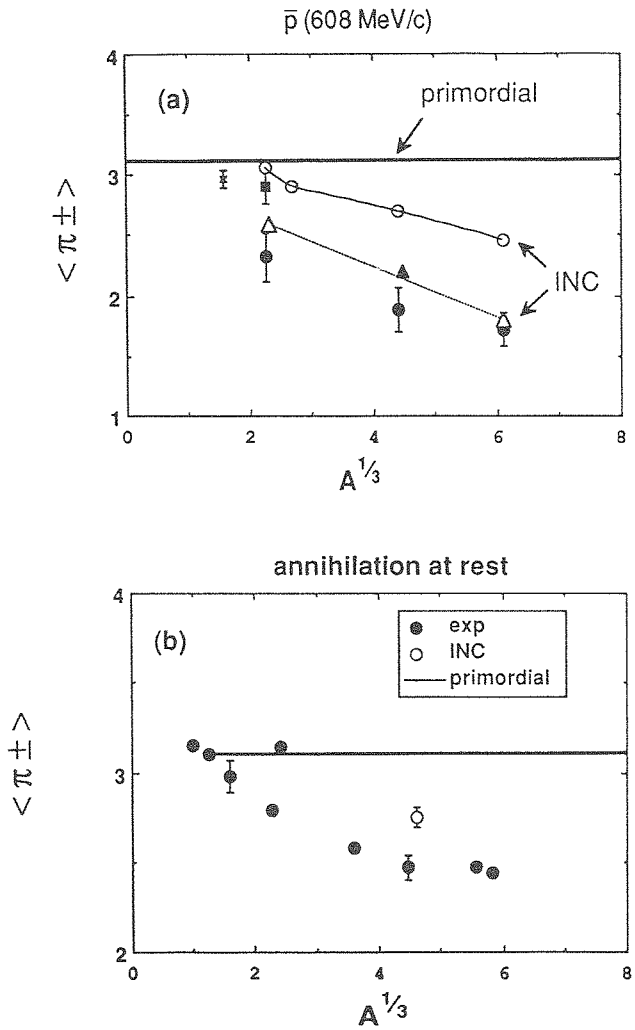

Fig. 16. Charged pion multiplicity for p̄-annihilation on various nuclei. The upper part refers to ~600 MeV/c antiprotons. The predictions of our standard INC calculations are shown by the open dots. The open triangles correspond to a modification of the $\Delta N \leftrightarrows NN$ cross section and of the Δ-lifetime given in the text. The primordial charged pion multiplicity is given for comparison. The experimental data are taken from ref. [3]) (full dots), ref. [50]) (cross), ref. [51]) (full square) and ref. [52]) (full triangle). In the lower part, the annihilation at rest is considered. The data (full dots) are taken from ref. [53]) (^{48}Ti, ^{181}Ta and ^{208}Pb), ref. [54]) (^{12}C), ref. [55]) (^{2}H), refs. [52,56-59]) (emulsion, the average is plotted) and ref. [60]) (^{14}N). See text for detail.

poorness of the data do not allow to extract L_0/λ and α_{int} with reasonable accuracy. Indeed, data are roughly consistent with a linear relation:

$$r_{\text{abs}} \approx \alpha_{\text{int}}(A)(L_0/\lambda)A^{1/3} = xA^{1/3} . \tag{4.3}$$

At rest, $x \approx 0.13$, while $x \approx 0.28$ at 600 MeV/c. If one takes the values predicted in

ref. [9]) and in this work for the average value of α_{int}: $\alpha_{int} \approx 0.40$ at rest and 0.60 at 600 MeV/c, one gets $L_0/\lambda \approx 0.32$ at rest and $L_0/\lambda \approx 0.47$ at 600 MeV/A, respectively. If L_0 is taken as the radius parameter, which amounts to assume that the average path inside the nucleus is equal to the nuclear radius, one gets an estimate of the (average) absorption mean free path. The results are $\lambda \approx 3.75$ fm at rest and ≈ 2.55 fm at 600 MeV/c. Note that these values are grossly consistent with the values extracted from π-induced reactions in the 100–300 range [34]). However, the absorption probability does decrease with increasing mass in the latter case.

4.3. COMPARISON WITH OUR STANDARD INC MODEL

The comparison is given in fig. 16a, which indicates that the INC model *considerably* underestimates the pion absorption (as defined by eq. (4.1)), especially for the light nuclei. For the π^-'s, measured in Ne target with streamer chamber, the disagreement is smaller, but nevertheless important. For annihilation at rest, the discrepancy seems to be ~20% [ref. [9])] (we did not have, for this process, a code which singles out charged states).

In the following, we try to determine the origin of this disagreement. It may come from one of the following causes: (i) the modification of the pion and delta properties inside nuclear matter; (ii) the inappropriateness of the pion creation and absorption mechanism (eq. (2.3)) used here; (iii) from the cascade model itself; (iv) from a possible modification of the annihilation mechanism. In the following, we investigate points (i)–(iii) successively.

4.4. MEDIUM EFFECTS

The situation looks roughly similar to the π-nucleus case where the INC model described here also underestimates the absorption [16]). Here we will proceed as in ref. [16]) and test the sensitivity of the model under variation of the dynamical input describing pion and delta interactions. The medium effects on several quantities (the $\Delta N \to NN$ cross sections e.g.) are not well known [35,36]). We therefore test the variation of the pion multiplicities under plausible modifications of the cross sections. We report in table 1 our results for some of these modifications. We tried many other ones, which did not bring interesting changes. We comment on some of them.

The first case in table 1 corresponds to a broadening of the $\pi N \to \Delta$ cross section, a modification which is consistent with the modification of the pion propagator inside nuclear matter. This does not appear very efficient to increase the pion absorption. The modification which seems the most efficient is a simultaneous increase of the $\Delta N \to NN$ cross section and of the Δ-lifetime. This is physically clear since in our model the π-absorption proceeds through the $\pi N \to \Delta$, $\Delta N \to NN$ sequence. A similar conclusion is obtained in ref. [16]), where the pion absorption on nuclei is investigated in detail. (The implications are discussed below.) We noticed

TABLE 1

Our standard INC results are given by the first line. The following modifications have been studied. (2): broadening of the $\pi N \to \Delta$ cross sections; (3) multiplication of the $\Delta N \leftrightarrows NN$ cross sections and of the Δ-lifetime by a factor 3; (4): narrowing of the primordial pion spectrum; (5): the same plus a reduction of the πN cross section above the Δ-resonance; (6): use of a mass-dependent Δ-lifetime; (7): modification (3) and use of the $\pi N \to \Delta$ cross section extracted from ref. [61]); (8): modification (3) with a reduction of the πN cross section above the Δ-resonance. The experimental data are given in (9). See text for more detail

		$\bar{p}+{}^{12}C$			$\bar{p}+{}^{238}U$		
		$\langle \pi_{abs} \rangle$	$\langle \pi^+ \rangle$	$\langle p \rangle$	$\langle \pi_{abs} \rangle$	$\langle \pi^+ \rangle$	$\langle p \rangle$
(1)	INC	0.3	1.32	1.35	1.21	0.89	4.29
(2)	broad $\sigma(\pi N)$	0.27	1.31	1.14			
(3)	$(\Delta N \leftrightarrows NN)\tau_\Delta(\times 3)$	0.50	1.21	1.11	2.10	0.72	4.81
(4)	narrow prim.	0.33	1.31	1.51			
(5)	$(4)+\sigma(\pi N)_{mod}$	0.43	1.29	1.32			
(6)	$\tau_\Delta(M)$	0.28	1.32	1.30			
(7)	$(3)+\sigma(\pi N)_{med}$				1.60	0.87	3.32
(8)	$(3)+\sigma(\pi N)_{mod}$				1.95	0.78	4.01
(9)	exp.		1.01 [a])			0.69 [a])	
			1.33 [b])				

[a]) Ref. [3]).
[b]) Ref. [51]).

however that the agreement for the proton spectrum is deteriorated with this modification, the tail decreasing then too slowly.

We also investigate the influence of the pion primordial spectrum, as in sect. 3.1. We used a spectrum similar to the one of McGaughey *et al.* [3]), noticeably narrower than our standard one. This does not modify the pion multiplicity, but increases the proton multiplicity. If a mass-dependent lifetime is introduced for the Δ, as in refs. [37,38]), nothing is really modified. We notice also that limiting the πN cross section to the Δ-bump (neglecting absorption above the resonance) generally decreases the absorption, as expected, but at the same time, gives a proton spectrum decreasing much too rapidly at large momentum.

4.5. MODEL FOR π-ABSORPTION

The observations made in sect. 4.4 seem to call for important medium effects. An alternative interpretation is that our pion absorption picture should be modified. The point is that the pion is absorbed through the two-step process: $\pi N \to \Delta$, $\Delta N \to NN$. This needs some time and therefore the time sequence may be important for pion absorption. This aspect can be investigated through a simple chemical model. Let us assume that a beam of pions always travelling along the z-direction falls on a semi-infinite matter ($z > 0$) and that these pions may transform under the

abovementioned reactions. Using a mean-free-path picture, one writes the following rate equations:

$$\frac{dn_\pi}{dz} = -\frac{1}{\lambda_f} n_\pi + \frac{1}{\lambda_d} n_\Delta , \tag{4.4}$$

$$\frac{dn_\Delta}{dz} = -\frac{1}{\lambda_f} n_\pi - \left(\frac{1}{\lambda_d} + \frac{1}{\lambda_a}\right) n_\Delta , \tag{4.5}$$

where $\lambda_d, \lambda_f, \lambda_a$ are the characteristic lengths associated with the Δ-decay, Δ-formation and the $\Delta N \to NN$ reaction, respectively. Here, we neglect the inverse reaction, which is negligible in this energy range. We also neglect the energy dependence of the various lengths; this feature is not expected to change our conclusion below. The solution of the system (4.4), (4.5) is rather straightforward for the initial conditions $n_\pi(z=0) = n_0$, $n_\Delta(z=0) = 0$. The absorption probability after a distance z is given by:

$$P_{abs}(z) = \left[\lambda_f \lambda_s \left(\frac{1}{\Lambda^2} - \frac{4}{\lambda_f \lambda_a}\right)^{1/2}\right]^{-1} \left[\frac{1}{\mu_2}(1 - e^{\mu_2 z}) - \frac{1}{\mu_1}(1 - e^{\mu_1 z})\right], \tag{4.6}$$

where

$$\frac{1}{\Lambda} = \frac{1}{\lambda_f} + \frac{1}{\lambda_a} + \frac{1}{\lambda_d} = \frac{1}{\lambda_f} + \frac{1}{\lambda}, \tag{4.7}$$

and where

$$\mu_{1,2} = \frac{1}{2}\left(-\frac{1}{\Lambda} \pm \left[\frac{1}{\Lambda^2} - \frac{4}{\lambda_f \lambda_a}\right]^{1/2}\right). \tag{4.8}$$

It is particularly instructive to compare (4.6) with the limit of vanishing total Δ-lifetime: $\lambda_a \to 0$, $\lambda_d \to 0$, λ_a/λ_d kept constant. In this limit the Δ's do not appear explicitly, although their properties dictate the branching ratios for pion absorption and pion quasi-elastic scattering. In this limit, the absorption probability becomes

$$P_{abs}(z) \to P_{lim}(z) = 1 - \exp\left(-\frac{\lambda}{\lambda_a}\frac{z}{\lambda_f}\right). \tag{4.9}$$

This formula is physically transparent. The probability of absorption per unit length dP_{abs}/dz is proportional to the probability of forming a Δ, multiplied by the branching ratio for the disappearance of the (implicit) Δ. With real Δ's (eq (4.6)), the absorption is reduced because the whole sequence takes some time. This is shown in fig. 17, for typical values of the λ-parameters. For small z, the absorption can be substantially smaller when the Δ-degrees of freedom are explicitly taken into account, compared to a calculation where only pions enter the model, even if the basic dynamical input is kept the same. This is the case for the calculations of refs. [4,5,39]). We will come back to this point.

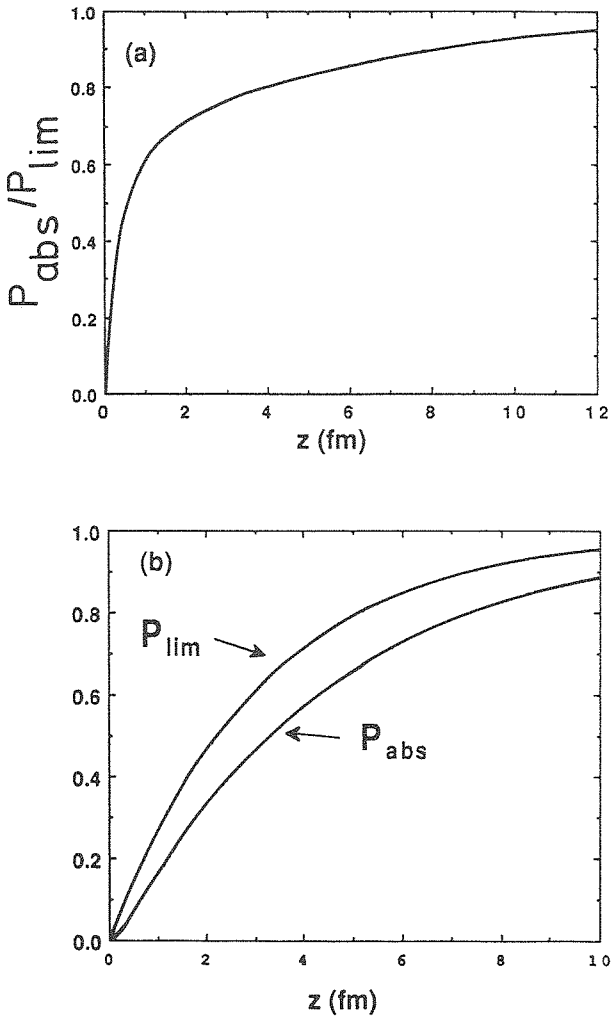

Fig. 17. Lower part: pion absorption probability P_{abs} after travelling a distance z inside nuclear matter, as estimated from eq. (4.6). The quantity P_{lim} corresponds to the limiting expression (4.9). The upper part gives the ratio P_{abs}/P_{lim}.

The relevance of the Δ-degrees of freedom has been demonstrated in the case of heavy-ion collisions [40]), to which the INC model is also applied. A well-defined peak has been identified in the invariant mass distribution for π^-p pairs, after a proper substraction of the background is performed. A similar analysis could easily be made in the antiproton–nucleus case. To provide a guideline, we give in fig. 18 the predictions of our INC model for the following observable

$$f(\sqrt{s}) = \frac{N_p(\sqrt{s})}{N_{unc}(\sqrt{s})}, \tag{4.10}$$

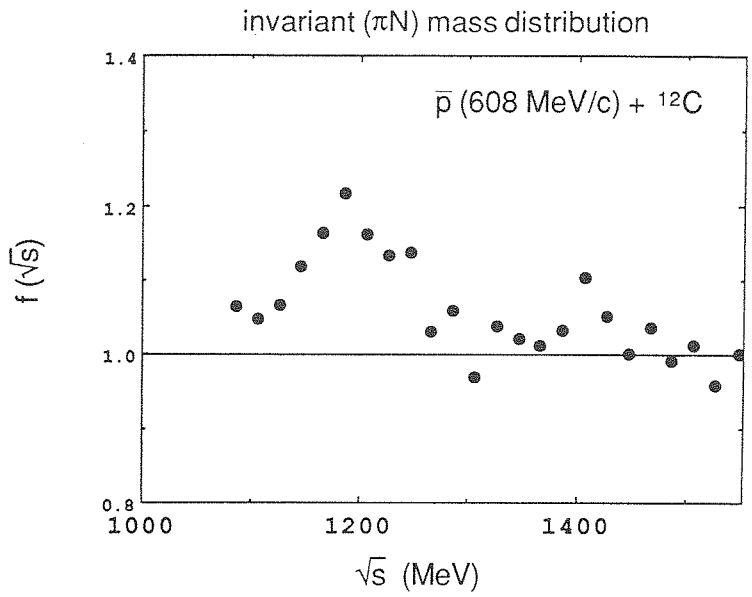

Fig. 18. Ratio (eq. (4.10)) between the invariant mass distribution for the correlated πN pairs and the one for uncorrelated pairs, as estimated by the INC model. See text for detail.

where N_p is the number of πN pairs with c.m. energy $\sqrt{s}$ and N_{unc} is the number of uncorrelated πN pairs at the same energy. The latter is constructed by picking up the pion and the nucleon at random in different events [41]). It is normalized as N_p for large $\sqrt{s}$, where no correlation occurs. In the actual calculation, the correlation peak lies a little bit below the average Δ-mass, because of kinematical selection of lower masses [42]).

4.6. THE INC AND THE MULTIPION DYNAMICS

One may wonder whether the observables discussed here are sensitive to the nonlinear aspects of the multipion dynamics. In other words, are they sensitive to the full development of the multipion cascade or are they merely given by the superposition of the individually and independently evolving pion cascades? We investigate this point in fig. 19, where we compare the results of our INC model to the results obtained when only one of the primordial pions chosen at random is retained. As for the pion cross section the difference is very small. It is a little bit more pronounced for the protons. This observation is in keeping with the analysis of refs. [31,43]), where the distributions of the particle multiplicities are analysed in terms of a clan picture, i.e. in a picture of independent but similar processes of particle production, initiated by the primordial pions.

Let us stress that observables like particle correlations definitely need be tackled by models including the full development of the multipion cascade.

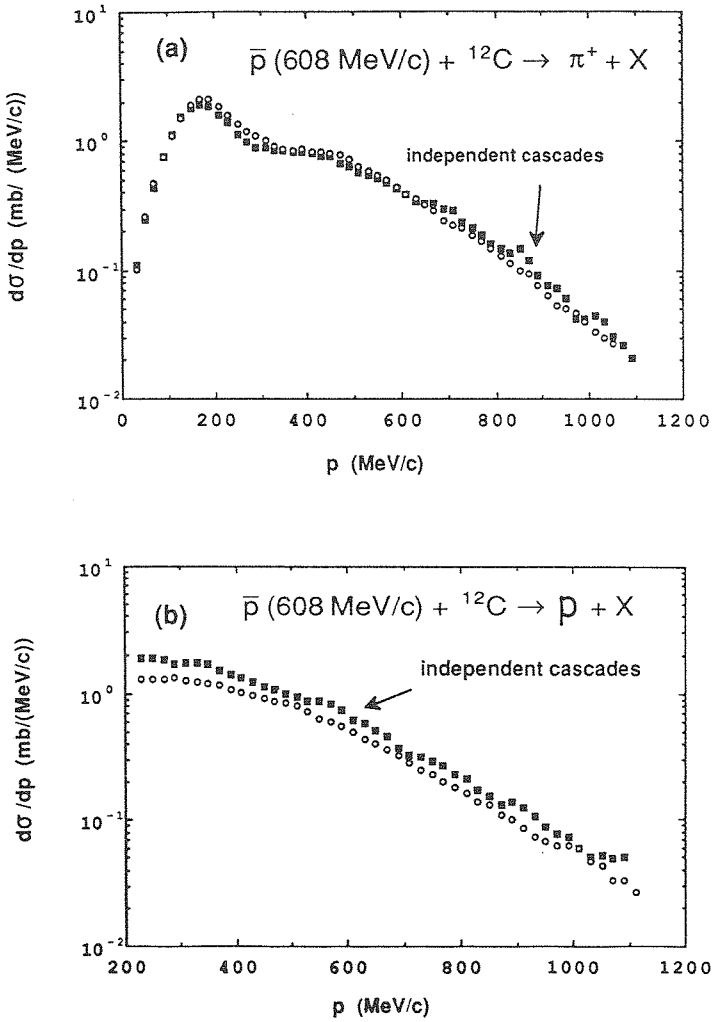

Fig. 19. Comparison between our standard INC results (open dots) and the results obtained by following one-pion cascade at a time. See text for detail.

4.7. CONCLUSION

We have pointed the extreme dispersion in the measurements of charged pion multiplicity for annihilation in flight. Nevertheless, it seems that there is some lack of absorption in our standard INC model. This lack may be attributed to possible medium effects on pion and especially on Δ-dynamics, although the modification required to account for the discrepancy is about the maximum size which can be accounted for by medium effects. We have seen that a modified pion absorption picture, eliminating explicitly the Δ-degrees of freedom increases the absorption yield. But, the presence of Δ's could be checked experimentally. Finally, the lack

of absorption does not seem to be related to the aspects of multipion dynamics introduced in our model.

5. Comparison between INC models

In order to clarify as much as possible the theoretical situation, we attempt a comparison between the INC models; more precisely, we concentrate the discussion on annihilation at 600 MeV/c, and perform a comparison of the works by McGaughey *et al.* [3]), Golubeva *et al.* [5]), Hernandez and Oset [39]) and ours. We will compare both the ingredients of the respective cascade models and the results. The prominent features of this comparison are schematically given in table 2.

TABLE 2

Comparison between INC models, concerning characteristic features (upper part) and results (lower part). All the numbers in the lower part refer to 600 MeV/c antiprotons except for those with a star, which correspond to ~500 MeV/c. The numbers in parentheses are quoted in ref. [5]) only. See text for more detail

		McGaughey *et al.* [a])	Iljinov [c])	Hernandez–Oset [d])	Our INC model	Exp.
primordial pion spectrum		too narrow	~OK	~OK	~OK	
σ_{ann}^{tot}		~OK		~OK	~OK	
pion cascades		"multi"	individual or multi	individual	multi	
pion absorption		two-step	mean free path	mean free path	two-step	
$\bar{p}+^{12}C$	$\langle\pi^+\rangle$	1.0	1.28 (1.18)*	1.16	1.32	1.01 [a]) 1.33 [b])
	$\langle p\rangle$		1.01 (2.06)*		1.35	1.58* [b])
	proton tail	too small	~OK		~OK	
$\bar{p}+^{238}U$	$\langle\pi^+\rangle$	0.65		0.79	0.93	0.69 [a])
	proton tail	~OK			~OK	

[a]) Ref. [3]). [b]) Ref. [51]). [c]) Refs. [4,5]). [d]) Ref. [27]).

There is no detailed information for the reliability of calculated total annihilation cross sections. Although one does not expect discrepancies of more than 20–30%, this is not without consequence when multiplicities are discussed. The generation of the primordial pions is said to be the same in all approaches. However, the primordial pion spectrum is obviously narrower than ours in McGaughey *et al.* [3]) (see ref. [2])). The cascade models differ in the way the pion cascades and the nonlinear effects are constructed. In McGaughey *et al.* [3]), the pion cascades are more or less independent, except that account for the depletion of the target seen by a cascading pion due to other pions is partly introduced, as described in ref. [44]). In the new version of the so-called Iljinov cascade (used in ref. [55])), the pion cascades are also

coupled through the depletion of the target: the so-called trawling effect. There is a difference between this work and the one of ref. [3]), even in the limit of independent cascades. Indeed in the work of ref. [3]), based on the Yariv and Frankel code [38,44]), a cascading particle creates holes in the density distribution. Therefore it experiences the depletion created by itself. It is also the case for our illustrative calculation explained in sect. 4.5, but not in the work of ref. [4]). In our opinion, this may explain why the "trawling" effect observed in ref. [5]) is (much) larger than the effect studied in sect. 4.5. In the paper by Hernandez and Oset [39]), the pion cascades are followed individually. In our work, all the particles are followed at the same time. The pion cascades are therefore coupled through the depletion of the target, but, moreover, the target is continuously readjusting, since all the target nucleons are moving. Furthermore, the Pauli blocking is instantaneously (and locally) applied. Concerning the pion absorption dynamics, the approaches divide into two classes: either they use mean free paths (refs. [5,39])) or they use the two step process $\pi N \to \Delta$, $\Delta N \to NN$ [ref. [3]) and our approach].

The McGaughey cascade yields a too small proton cross section, especially for the ^{12}C target. This has been interpreted as a proof for frequent annihilations on two nucleons [27]) or as due to the formation of a cold quark-gluon plasma [26]). We have shown that the proton tail is intimately connected to the one of the primordial pion spectrum. In ref. [3]), the latter decreases too fast, this opinion being shared by the authors themselves (see last sentence of p. 2157). The absorption is underestimated by all the calculations except the one of ref. [3]) (if the McGaughey data for ^{12}C are retained). The difference between the three other works can be more or less understood from the discussions of sects. 3 and 4. But the difference between the McGaughey results and ours still remain a puzzle for us and call for a detailed comparison between the two codes.

6. Discussion and conclusion

We have here analyzed many details of the INC model, applied to the antiproton-nucleus annihilation. We want to point out the most significant results of our analysis and discuss their implications.

First, the main features of the pion and proton spectra are easily described by any cascade model. For the pion spectrum, this seems to come from the fact that the high-energy tail is largely dominated by the noninteracting pions, whose spectrum is well known (at least in free space), and that the low-energy part is dominated by the interacting pions, whose distribution is quite broad also. Details are also more or less understood. The question of the proton spectrum is a little bit more difficult. The amplitude of the tail is basically determined by the tail of the pion spectrum and by the detail of the interaction for high-energy pions (above the Δ-resonance). The overall normalization of the proton spectrum has not received enough attention. In particular, the relation between the proton multiplicity and the energy transferred

from the pion system to the nucleon system would be worth to investigate in more detail, for this feature is also influenced by the pion dynamics.

The second aspect deals with the correlations between various observables. As we have said, these quantities should be described by models involving multipion propagation and interactions. Unfortunately, the only existing data seem to reveal only correlations dictated by conservation laws and not yet dynamical correlations. We have underlined the necessity to look at pion–proton invariant mass correlations.

A key quantity seems to be the pion multiplicity. Fragmentary information is available as far as energy and charge dependences are concerned. The only existing systematic concerns the $\pi^{\pm}$ multiplicity at 600 MeV/c. It includes several targets but is blurred by large uncertainties. From the theoretical point of view, the results are rather scattered. Nevertheless, except for the calculation of ref. [3]) one can say that the absorption is underpredicted theoretically. We have mentioned several ways of investigation in order to improve this situation:

(i) possible medium effects can increase the absorption. However, the size necessary to achieve good agreement is rather unrealistic;

(ii) the removal of the explicit Δ-degrees of freedom goes in the right direction. Let us stress that the influence of these degrees of freedom is not eliminated necessarily. The latter may be reflected in the energy dependence of the mean free paths discussed for instance in sect. 4. This is the approach followed by the authors of refs. [5,39]), where some medium effects (broadening of the Δ-bump in the πN cross section e.g.) are taken into account. We have indicated an experimental test to find out the presence of the Δ-reasonances in the reaction process.

Other possible effects can be looked for:

(i) pion absorption on several nucleons. It is however hard to distinguish, at least in model of ref. [39]) and ours, between genuine absorption on two or more nucleons and rescattering;

(ii) presence of meson resonances. It is well known that antiproton–proton annihilation produces meson resonances ($\eta, \rho, \omega, \ldots$). The latter are ultimately detected as pions (except possibly for η). They have different absorption properties than their pion content. It is not known, however, whether this could increase or decrease the apparent pion absorption.

(iii) annihilation on several nucleons. This kind of process may not be so unfrequent, as theoretical studies indicate [17,45,46]) and as it can be seen directly from the existence of the process [47,48]) $\bar{p}d \to \pi^- p$. For the annihilation on heavier nuclei, the existence of this process is not yet completely demonstrated, but rather convincing analyses [17]) indicate that it could occur 20–30% of the time. The influence on pion multiplicity is still uncertain, for it depends upon the mechanism for the annihilation. At least two models have been proposed. In ref. [49]), it is assumed that in antinucleon–nucleon annihilation a pion is produced off-shell which is reabsorbed by another nucleon. In this model, the number of primordial pions is decreased by one unit compared to usual annihilation events. Another model has been proposed pre-

viously [45]) which basically assumes a phase space model for the decay of a ($\bar{N}NN$) system into a nucleon plus any number of pions. According to ref. [46]), the number of primordial pions is reduced by $\sim\frac{1}{3}$ of a pion.

We are currently investigating the last two possibilities in more detail.

In conclusion, we have seen that many important aspects of the existing data for in flight annihilation nuclei in the LEAR regime are not fully understood. This situation points to an urgent need for new measurements and clarifying theoretical calculations.

We are grateful to Drs. G. Bendiscioli, C. Guaraldo, E. Hernandez, D. L'Hôte, E. Oset, G.A. Smith and P. Truöl for helpful discussions. We want to thank Dr. T. Bressani for providing us with antineutron data prior to publication.

References

1) J. Cugnon, Proc IX European Symp on Antiproton-proton interactions and fundamental symmetries, Mainz, 1988, Nucl. Phys. B [Proc. Suppl.] **8** (1989) 225
2) M.R. Clover, R.M. De Vries, N.J. Di Giacomo and Y. Yariv, Phys. Rev. **C26** (1982) 2138
3) P.L. McGaughey *et al.*, Phys. Rev. Lett. **56** (1986) 2156
4) A.S. Iljinov, V.I. Nazaruk and S.E. Chigrinov, Nucl. Phys. **A382** (1982) 378
5) Ye S. Golubeva, A.S. Iljinov, A.S. Botvina and N.M. Sobolevsky, Nucl. Phys. **A483** (1988) 539
6) M. Cahay, J. Cugnon and J. Vandermeulen, Nucl. Phys. **A393** (1983) 237
7) J. Cugnon and J. Vandermeulen, Nucl. Phys. **A445** (1985) 717
8) J. Cugnon, P. Jasselette and J. Vandermeulen, Nucl. Phys. **A470** (1987) 558
9) P. Jasselette, J. Cugnon and J. Vandermeulen, Nucl. Phys. **A484** (1988) 542
10) D. Garreta *et al.*, Phys. Lett. **B149** (1984) 64
11) D. Garreta, in "Antinucleon- and nucleon-nucleus interactions", ed. G.E. Walker *et al.* (Plenum, New York, 1985)
12) F. James, CERN Yellow Report 68-15
13) R. Stenbacka *et al.*, Nuovo Cim. **51A** (1979) 63
14) J. Vandermeulen, Lett. Nuovo Cim. **11** (1974) 243; **21** (1978) 33
15) D. L'Hôte, thesis, unpublished
16) J. Cugnon and M.-C. Lemaire, Nucl. Phys. **A489** (1988) 781
17) J. Cugnon, in The Elementary Structure of Matter, ed. J.M. Richard *et al.* (Springer, Berlin, 1988) p. 211
18) P.L. McGaughey, M.R. Clover and N.J. DiGiacomo, Phys. Lett. **B166** (1986) 264
19) A. Angelopoulos *et al.*, Phys. Lett. **B205** (1988) 590
20) Particle Data Group, Phys. Lett. **B204** (1988) 1
21) S. Frankel *et al.*, Phys. Rev. **C18** (1978) 1375
22) S.A. Gurvitz, Phys. Rev. Lett. **47** (1981) 560
23) M. Avan *et al.*, Phys. Rev. **C37** (1987) 231
24) P. Grangé, J. Cugnon and A. Lejeune, Nucl. Phys. **A473** (1987) 365
25) S. Fantoni and V.R. Pandharipande, Nucl. Phys. **A427** (1984) 473
26) J. Rafelski, Phys. Lett. **B207** (1988) 371
27) E. Hernández and E. Oset, Nucl. Phys. **A493** (1989) 453
28) F. Balestra, Nucl. Phys. **A491** (1989) 541
29) R. Hagedorn, Nucl. Phys. **B24** (1970) 93
30) T. von Egidy *et al.*, Physics at LEAR with low energy antiprotons, ed. C. Amsler *et al.* (Harwood Acad. Publ., Chur, 1988) p. 729
31) J. Cugnon, P. Deneye and J. Vandermeulen, Phys. Rev. **C38** (1988) 795

32) H.J. Besch *et al.*, Z. Phys. **A292** (1979) 197
33) T. Bressani *et al.*, Proc. of the few body problems, Workshop, Prague, to be published
34) D. Ashery *et al.*, Phys. Rev. **58** (1987) 463
35) B. ter Haar and R. Malfliet, Phys. Rev. **C36** (1987) 1611
36) R. Cenni and G. Dillon, Nucl. Phys. **A422** (1984) 527
37) Y. Kitazoe *et al.*, Phys. Lett. **B166** (1986) 35
38) Y. Yariv and Z. Fraenkel, Phys. Rev. **C20** (1979) 2227
39) E. Hernández and E. Oset, Nucl. Phys. **A455** (1986) 584
40) J.-P. Alard *et al.*, Diogene Meeting, Gif-sur-Yvette, June 1988
41) W.A. Zajc *et al.*, Phys. Rev. **C29** (1984) 2173
42) J. Cugnon, D. Kinet and J. Vandermeulen, Nucl. Phys. **A352** (1981) 505
43) J. Cugnon, P. Jasselette and J. Vandermeulen, Europhys. Lett. **4** (1987) 535
44) Y. Yariv and Z. Fraenkel, Phys. Rev. **C29** (1981) 488
45) J. Cugnon and J. Vandermeulen, Phys. Lett. **B146** (1984) 16
46) J. Cugnon and J. Vandermeulen, Phys. Rev. **C39** (1989) 181
47) R. Bizarri *et al.*, Lett. Nuovo Cim. **2** (1969) 431
48) G.A. Smith, The elementary structure of matter, ed. J.-M. Richard *et al.* (Harwood Acad. Publ. Chur, 1987) p. 703
49) E. Hernández and E. Oset, Phys. Lett. **B184** (1987) 1
50) F. Balestra *et al.*, CERN-EP/87-213
51) L.E. Agnew *et al.*, Phys. Rev. **118** (1960) 1371
52) A.G. Eksprong *et al.*, Nucl. Phys. **22** (1961) 353
53) G.T. Condo *et al.*, 4th Int. Symp. on antinucleon-nucleon interaction, Syracuse (1975), p. VI-11
54) M. Wade and V.G. Lind, Phys. Rev. **D14** (1976) 1182
55) T. Kalogeropoulos and G.S. Tzanakos, Phys. Rev. **D22** (1980) 2585
56) O. Chamberlain *et al.*, Phys. Rev. **113** (1959) 1615
57) H. Barkas *et al.*, Phys. Rev. **105** (1957) 1037
58) E. Amaldi *et al.*, Nuovo Cim. **14** (1959) 977
59) A. Berthelot *et al.*, Nucl. Phys. **14** (1960) 545
60) J. Riedlberger *et al.* (Asterix Collaboration), Mainz Conf. on antinucleon-nucleon interactions, 1988
61) E. Oset, L.L. Salcedo and D. Strottman, Phys. Lett. **B165** (1985) 13